

# Nonlinear Behavior of Irregularly Shaped Reinforced Concrete Buildings with Different X-Bracing Positions

Marwa Bakhouché<sup>1\*</sup>, Rafik Madi<sup>1</sup>, Moufida Gherdaoui<sup>2</sup>

<sup>1</sup> Civil Engineering and Hydraulics Laboratory, University 8 Mai 1945, P.O. Box 401, Guelma, Algeria

madi.rafi@univ-guelma.dz<sup>1</sup>

<sup>2</sup> Department of Civil Engineering, University Abbès Laghrou P. O. Box 1252, Khenchela, Algeria

Corresponding author<sup>1\*</sup>: E-mail: bakhouché.marwa@univ-guelma.dz

Received: 25-03-2023

Accepted: 05-05-2023

Published: 15-05-2023

## Abstract

Horizontally irregular structures are popular in modern urban design due to aesthetics and the limited availability of land. Horizontal irregularities may improve the structure's architectural appeal but might substantially impact its performance. Previous research has demonstrated that buildings with irregular configurations are destroyed by significant ground motion. Bracings are a common method for ensuring structural safety during significant earthquake occurrences. These bracings can be placed in different positions in a structure. In this context, the present study aims to determine the most effective position of X-bracing configuration which can be used to minimize the damage of horizontal irregular shape structures. In this study, irregularly shaped RC structures are investigated with and without steel bracings in different positions in frames. The nonlinear static analysis is performed for all the models. All the modeling, design, and analysis are performed in ETABS. The results are reported in terms of Maximum story displacements, inter-story drifts, base shear, Fundamental time periods, story stiffness, torsional irregularity, capacity curves, and plastic hinge formations. The results indicate that, if the position of the bracing in the frames is properly considered, the steel bracing is effectively used as retrofitting process in buildings of irregular shapes.

**Keywords:** Irregular buildings, Steel bracings, Horizontal irregularities, Nonlinear static analysis, ETABS software, Seismic retrofitting.

**Tob Regul Sci.™ 2023;9(1): 1875-1904**

**DOI: doi.org/10.18001/TRS.9.1.130**

## Introduction

The distribution of stiffness, mass, plane, strength, and many other irregularities in the vertical and horizontal orientations of the building all affect how the structure reacts to an earthquake. Previous cases of building destruction have shown that irregularity is a crucial factor in the failure of a structure during strong earthquakes. When a building is exposed to an earthquake, the structure

generates horizontal forces, which result in inertial forces acting through the center of mass of the structure. Vertical walls and columns resist all of these forces, and the combined effect of these forces acts through a point called the center of rigidity. The amount of horizontal and vertical irregularities significantly impacts a structure's performance under severe earth shakes. Excitations due to earthquakes endanger existing structures. Designing structures for their seismic susceptibility is of utmost importance as it affects socio-economic losses. The behavior of structures during a seismic event differs considerably from that of wind loads and usually results in elastic deformation of the same structures. The perfect irregularity of buildings is thought to be a phenomenon of idealization. The major national and international code provisions imply that the regularity of plans and elevations is the result of two distinct points of view, but in reality, it is the result of the combination of these two points of view. A paradigm shift has already occurred in the differential examination between irregular and regular structures. The irregularity of planes suggests that this type of asymmetric behavior is caused by a non-uniform distribution of mass, stiffness, and strength throughout the building, resulting in significant story rotations (torsional response) and story displacements. Previous earthquakes confirm this theory.

Architectural plans of various shapes, including L, T, H, C, and plus-shaped structures, are the most common horizontal irregularities. Torsional irregularities, diaphragm irregularities, re-entrant corner irregularities, and massive holes are examples of the new types of horizontal irregularities. These structures' centers of mass and stiffness are not aligned, resulting in excessive torsion and structural damage [35]. Standards for serious structural irregularities and regulations for dealing with potential irregularities must be established to analyze irregular structures. Drift, structural displacement, and story shear all affect the structure. RPA99/2003 (Algeria), EC 8 (Europe), ASCE7 (USA), and IS 1893 (India) are the codes used to deal with seismic loads [13].

Due to various factors, such as a change in guidelines, a modification of the type of building use, the introduction of additional floors in the construction, or an absence of sufficient strength in the concrete, the rigidity and strength of the construction are insufficient in some buildings, and therefore the retrofitting of the building becomes necessary. These buildings need to be retrofitted to meet changing conditions and comply with regulations. Various seismic factors, such as force reduction factor, overstrength factor, ductility, period, and so on, must be known to retrofit a building. There are several methods for retrofitting an existing RC building, including the use of FRP laminates, concrete or steel jacketing, adding shear walls, and steel bracing. So even though reducing a building's global displacements is an important factor in reducing the extent of failure during an earthquake, steel bracing of RC buildings, as a global method of retrofitting, is a very suitable technique to decrease the global displacement, reduce displacement ductility demand, and increase the building's capacity. Steel bracing can be attached to an existing RC frame in three ways: to an exterior face of the frame, inside an individual unit frame and attached to the frame via an intermediary steel frame, or the brace can be placed inside the frame and directly connected to the RC frame [9]. The first solution has several disadvantages, including architectural constraints, eccentric load transmission between the strut and the RC frame, and difficulties in

attaching the strut to the frame. The second strategy also has some disadvantages, such as cost and difficulty in connecting the intermediate steel frame to the RC frame. The third approach, known as direct internal bracing, does not have the disadvantages of the other two and has been widely used to retrofit RC frames. Maheri and Sahebi [31, 32] were the first to suggest this strategy. They presented the results of tests on scaled RC frames equipped with steel X-bracing directly attached to the frames. The test results showed that the bracing method can significantly increase the shear strength of RC frames.

Several studies have been conducted on retrofitting RC frames with concentric and eccentric steel bracing systems. Maheri and Fathi [30] studied the seismic performance of two-dimensional RC frames with three alternative X-bracing configurations: centrally stacked (C), end-stacked (E), and diagonally distributed (D). Nonlinear pushover analyses were performed on several retrofitted and non-retrofitted frames. They found that the diagonally distributed bracing configuration (D) had the best overall seismic performance of the retrofitted RC frames. Viji et al. [11] studied the performance of the building when the bracing is eccentric, as well as the performance of the structure with a mega-braced frame. According to the results, the bracings reduced the column's lateral displacement and bending moment. Pervez et al. [21] conducted an experimental study on retrofitting a structure with weak beam-column joints using eccentric inverted "V" type steel braces to prevent brittle failure at the beam-column joints. They concluded that the performance of the braced frame was better than the as-built RC frame. Bohara et al. [17] analyzed L-shaped RC structures with and without inverted V-shaped steel bracing at different frame locations, using ETABs software for response spectrum analysis. It was found that the installation of steel bracing effectively reduces the inter-story drift and displacements of the structure. Tehrani and Salari [40] examined the seismic performance of four different irregular RC structures with two different plane configurations, strengthened by steel bracing in X and zigzag configurations, as well as the seismic design and evaluation of structural models using linear and nonlinear static and dynamic analyses. The results could lead to a significant increase in the seismic performance of structures, as well as demonstrate that the seismic performance of models evaluated with simultaneous irregularities in plane and height was adequate. Castaldo et al. [39] studied the efficacy of BRBs for seismic retrofit of reinforced concrete (RC) structures with masonry infills, utilizing both non-linear static and incremental dynamic models using real ground motion recordings. The findings offer insight into the influence of BRBs and infill walls on the seismic performance of the system's various components and the effectiveness of a BRB retrofit for a real-world case study. Formisano et al. [3] studied the seismic vulnerability of reinforced concrete structures built to support gravity loads and updated with concentric exterior steel bracing systems. The seismic performance was tested using the so-called N2 approach in the style of the capacity spectrum method. The results demonstrated the importance of infills in the structural behavior of existing structures, as well as the effectiveness of exterior steel bracing systems as an upgrade strategy for existing RC buildings. Rahimi and Maheri [8] studied the impact of retrofitting RC frames with X-bracing on the seismic performance of existing RC columns using a numerical model. They concluded that retrofitting low-rise RC

frames with steel X-bracing improves the performance of the columns in almost all respects; however, for medium- and high-rise frames, the negative effects of retrofitting, especially on the columns attached to the bracing system, are significant, and in some cases, local reinforcement of the columns before the application of the bracing system may be necessary. Saji and Lekshmi [46] investigated the seismic analysis of chevron bracing in regular and irregular structures using G+14 buildings of different layouts. Response spectrum analysis was performed.

Therefore, a nonlinear static procedure (NSP) has been used for effective seismic demand estimation in building design. For the direct assessment of plastic deformation requirements in ductile materials and strength estimation, NSP approaches are employed. Among the methods used to assess structures under seismic stresses are pushover analysis and the streamlined single spectral mode elastic approach. To get a decent approximation of the total deformation response, these techniques have been used for the study of small structures utilizing just the first mode response or for a single-degree-of-freedom (SDOF) model [24]. Ganaie et al. [26] investigated seismic parameters such as maximum story displacements, inter-story drift, base shear, capacity curves, and failure behaviors using the response spectrum analysis and pushover analysis in four-story soft-story irregularity structures retrofitted with inverted V shape steel bracing using ETABS software. The results reveal that adding steel bracings successfully boosts the strength and stiffness of the constructions. Krishnan and Thasleen [37] used Pushover analysis to evaluate the responses of 10 re-entrant corner irregular structures. The acquired findings are compared to those of a regular structure.

This study aims to find the most effective positions of the X-bracing configuration for minimizing the response of a 12-story irregular RC structure. For this purpose, sixteen different models are modeled in ETABS (2018). Nonlinear static analysis is performed for all the models to understand the effect of different positions of X-bracing configuration on the overall response of the structures.

### **Irregularity of the buildings**

Buildings that are not symmetrical and have discontinuities in mass, shape, load-bearing elements installed in the structure, or material qualities of the individual elements are referred to as irregular [23]. Due to these imperfections, the center of mass and the center of stiffness of the structure are not congruent, resulting in large torsional forces [6]. Based on the physical discontinuities in elevation, plan, or both, structural irregularities in civil engineering can be divided into horizontal and vertical categories of irregularities, as illustrated in Figure 1. The performance of the structure under lateral seismic forces is affected by this discontinuity [36].

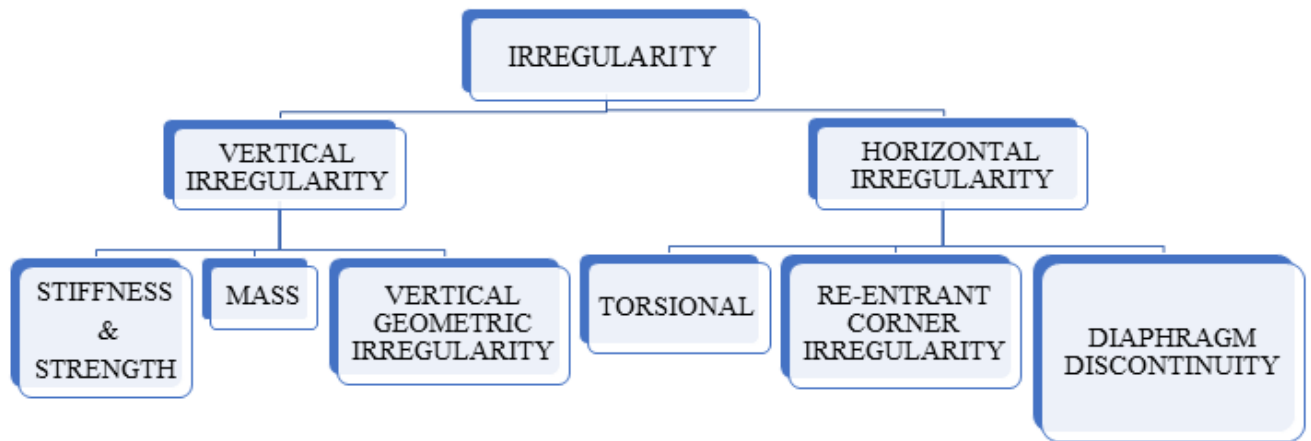


Fig. 1. Irregularity of buildings

### Horizontal Irregularity

Any discontinuity in the horizontal resisting parts, such as wide openings, cuts, or re-entrant corners, is referred to as horizontal irregularity in a structure. Asymmetrical building designs of various forms, such as L, T, F, U, O, and so on, fall under this category. These alterations result in stress concentrations, torsion, and diaphragm deformations [7].

- **Vertical Irregularity**

When a structure's stiffness, strength, or mass distribution abruptly changes along the height of the reference structure, it is referred to as having a vertical irregularity [2].

- **Seismic Performance of Irregular Structures**

The seismic performance of building systems is significantly influenced by the analysis approach used. The main purpose of structural analysis is to obtain the behavior of a structure when subjected to a load, such as live load, dead load, wind, or vibrations due to an explosion, earthquakes, and so on [12].

- **static Seismic Methods**

Due to their simplicity and ease of implementation, static analysis methods have been widely adopted [4]. Static methods often rely on substituting the idea of inertial forces at the stories of the structure with horizontal forces equal to the weight of the structure plus its acceleration. The sum of these concentrated forces is represented by the shear at the base of the structure [14]. The static analysis methods are divided into two categories: linear analysis, which may be utilized for regular structures with a limited height, and non-linear analysis, which takes into account the structure's inelastic behavior and is thus preferable to dynamic or linear static analysis. The equivalent static analysis/equivalent lateral force process, sometimes referred to as seismic coefficient methods, makes up the linear portion, while the pushover analysis method makes up the non-linear portion [38, 44].

- **Pushover Analysis Method**

Pushover analysis is a modified nonlinear static process used to predict structural deformations that have gained popularity among structural engineers due to the dependence of performance-based

design on nonlinear static methods. The foundation of nonlinear static processes is the transformation of a multi-degree-of-freedom (MDOF) system into an equivalent single-degree-of-freedom (SDOF) system, from which estimates of maximum displacement, story drifts, and other principal components can be obtained. Furthermore, the pushover or capacity curve used to build the corresponding SDOF model may be utilized to calculate structural capacity [1, 41].

- **Dynamic Seismic Methods**

Due to their ease of implementation, static analysis approaches have dominated in recent years. With the development of computer devices and analysis programs, researchers have created dynamic analysis methods that use simulated building models to examine the effect of earthquakes using a realistic seismic response. The analysis is based on logical reasoning and solving difficult mathematical equations [12]. Dynamic analysis is recommended for irregular structures with irregular mode shapes, i.e., all frame buildings with heights greater than 12 m in high seismic zones and greater than 40 m in medium seismic zones, according to existing codes in the field. These techniques are further subdivided into linear dynamic analysis,

Response spectrum analysis and linear time history analysis. When applying higher modes of vibration and the real distribution of forces in the elastic range, the approach demonstrates an improvement in analysis. The degree of force and its distribution along the height of the structure is the key difference between static and dynamic analysis [38]. The Non-linear time history analysis, incremental dynamic analysis, and non-linear response history analysis are all included in the non-linear dynamic section. The dynamic analytic approaches accurately represent the structure's real behavior during an earthquake [38, 44, 14].

- **Response Spectrum Analysis Method**

The response spectrum technique, also known as the mode superposition method or modal method, is an established method for the dynamic analysis of buildings [44]. The response spectrum (RS) technique is a commonly used approach for building design and seismic structural response calculation that uses vibrational waves or mode shapes [43]. Using modal combination methods such as absolute sum (ABS), square root sum of squares (SRSS), or full quadratic combinations (CQC), as illustrated in equations 1, 2, and 3, the responses of distinct modes are combined to obtain an estimate of the overall structural response:

$$R_{max} = \sum_{i=1}^n |R_i| \quad (1)$$

$$R_{max} = \sqrt{(\sum_{i=1}^n R_i^2)} \quad (2)$$

$$R_{max} = \sqrt{(\sum_{i=1}^n \sum_{j=1}^n R_i P_{ij} R_j)} \quad (3)$$

Where ,

$R_{max}$  is the estimated maximum response for quantity  $R$ ,  $R_i$  is the maximum response of  $R$  quantity in mode  $I$ , and  $n$  is the number of modes considered,  $\omega_i$ ,  $\beta_i$ ,  $\omega_j$ , and  $\beta_j$  are the natural frequency and critical damping ratio for  $i^{th}$  and  $j^{th}$  modes, respectively.

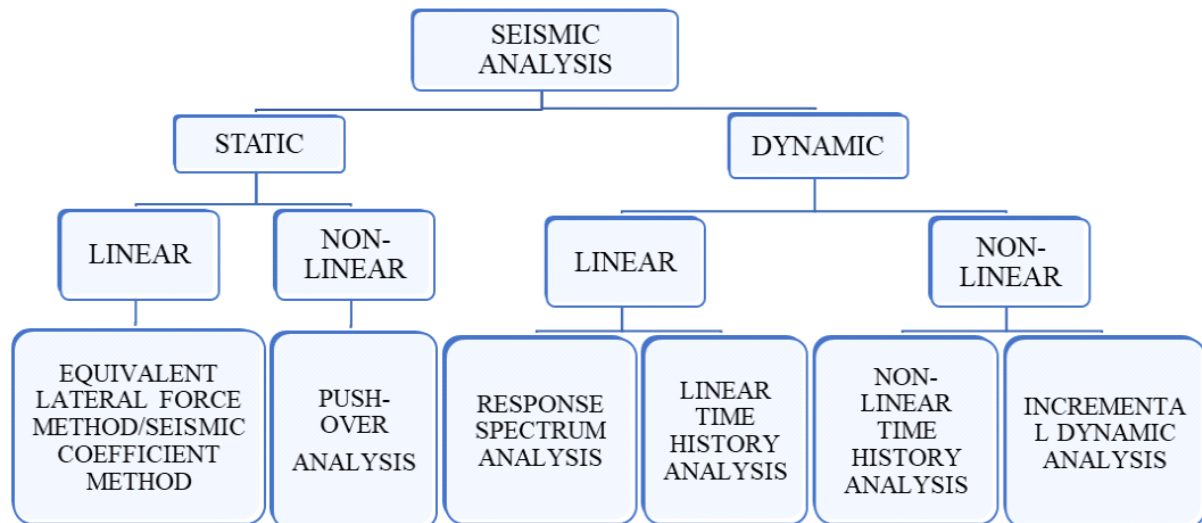


Fig. 2 seismic analysis methods types.

### Methodology and Modelling details

- **Modelling details**

To examine the effectiveness of different positions of steel X-bracing in existing irregularly shaped RC buildings, we suggest a hypothetical 12-story irregularly shaped building constructed as a moment-resisting frame. In plan, the structures have an irregular shape that resembles I, T, L, and Plus shapes (Fig. 3). The buildings have an average story height of 3.06 m, which is the usual height in Algeria. The total height of the building is 36.72m. Each span is assumed to be 5m wide, i.e., the span from one column to another is 5m, as shown in Fig. 3 in the x and y directions. Table 2 shows the cross-sections of the beam and columns. The slab thickness is 200mm, and the slab is considered a rigid diaphragm (Sukrawa, 2017) [33]. The materials properties used are given in Table 1. The concrete used in the columns, beams, and slabs is intended to have a compressive strength of 25 MPa, and the reinforcing bar grade is S235. Hollow square cross-section steel bracing is used in this study, and the bracings are used in different bays, as shown in Table 3 (thick bays in bold represent the locations where steel bracing is used). Table 2 shows the different plans of buildings with different locations of bracings (thick bays in bold) and a 3D view of the corresponding model. Nearly 16 models are observed and each model is named M1 to M16, with M1, M5, M9, and M13 being the original unbraced model for 12-stories buildings. The rest of the models represent structures with different locations of X-steel bracing, as shown in Table 2. The Algerian seismic standard RPA99/2003 [42] is utilized for seismic design, while Eurocode 2 is used for concrete building design [19]. The building stories are designed for a live load of 6.1 kN /m<sup>2</sup> and for the top story considered to be 6.5 kN /m<sup>2</sup> and for the dead load of 1.5 kN /m<sup>2</sup> and 1 kN /m<sup>2</sup>, respectively. The seismic behavior of irregularly shaped structures without and with different locations of X-steel bracing is investigated using the finite element program ETABS [25]. For seismic design reasons, the building is considered to be in Algeria, and the Algerian seismic design code is used in this study. The building is in seismic zone III, with a damping ratio of 5%. Firm soil S2 is the soil type, while Groupe 2 is the importance class. For the Special moment-

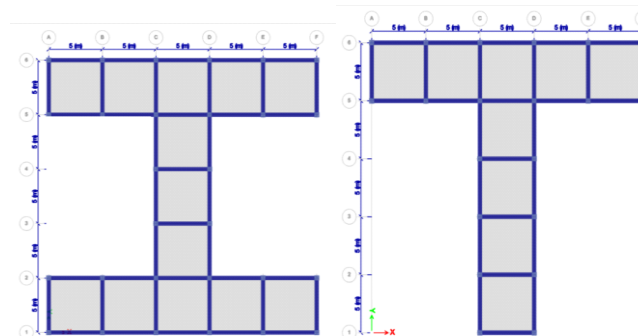
resisting frame (SMRF) construction system, the structural force reduction factor is  $R=5$  [42]. Some assumptions are established for the seismic design of the structure such that the P- $\Delta$  effect is evaluated for each model for response spectrum analysis (RSA). The model does not take into account the soil-structure interaction, and the base is restrained in three directions: X, Y, and Z. The RSA takes into account SSRS (square root of the sum of squares) and CQC (Complete Quadratic Combination). According to RPA99/2003, a sufficient number of modes are considered in the study so that the sum of all model masses for all modes assumes 99% of the total seismic mass.

**Table 1: Properties of the steel and concrete materials**

Material properties	Concrete	Grade	C25/30
		Modulus of elasticity	31000 MPa
		Poisson ratio	0.2
		Density	2500 Kg/m <sup>3</sup>
		Stress-strain diagram	Fig.4a
	Steel bracing	Grade	S235
		Modulus of elasticity	210000 MPa
		Minimum yield stress	235 MPa
		Minimum tensile strength	360 MPa
		Poisson ratio	0.3
		Density	7850 Kg/m <sup>3</sup>
		Stress-strain diagram	Fig. 4b

**Table 2: Specifications of beams, columns, slab, and bracing used in the 12-story study buildings**

RC sections			Steel bracing section (hollow section in mm)
Columns (cm)	Beams (cm)	Slab (cm)	200x200x12
45x45	35x35	20	





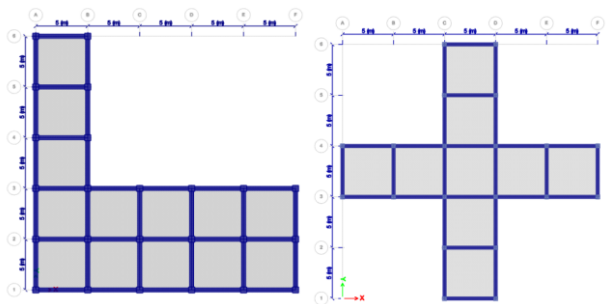


Fig. 3 Plan view of I, T, L, plus-shaped buildings

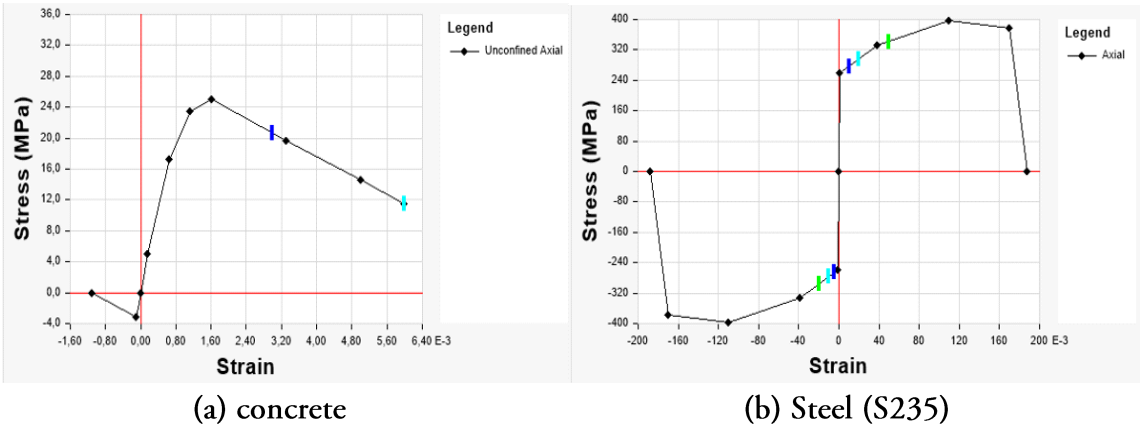
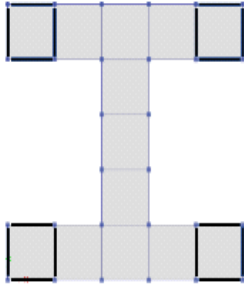
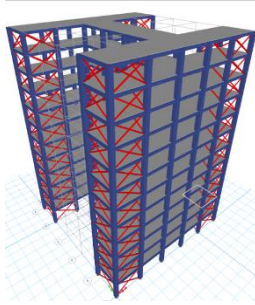
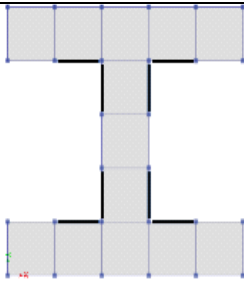
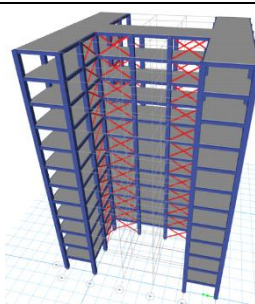
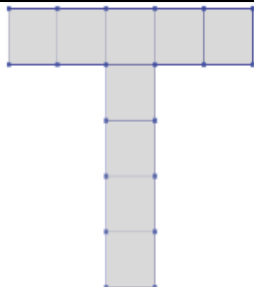
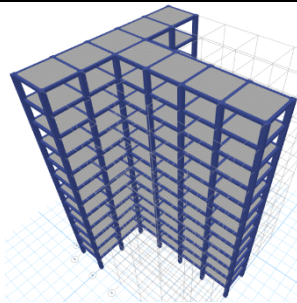
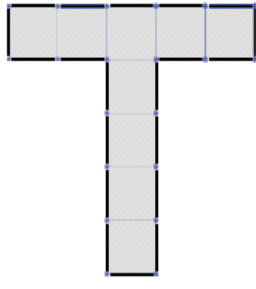
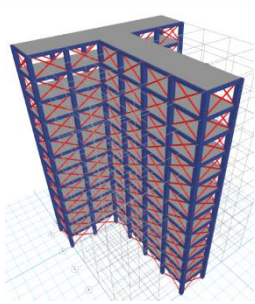
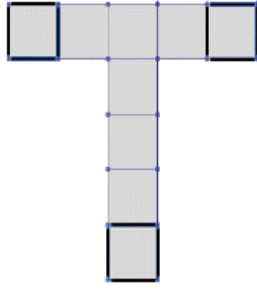
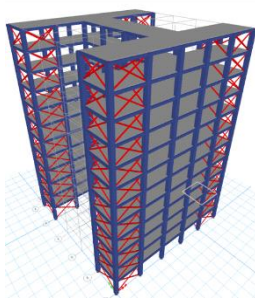
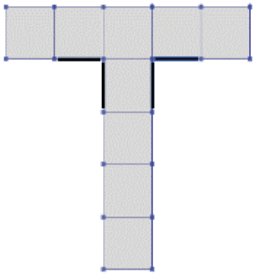
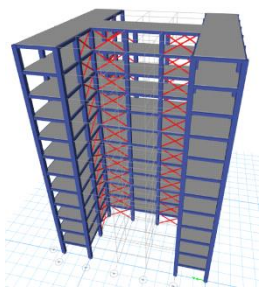
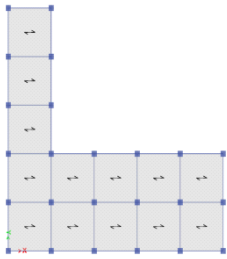
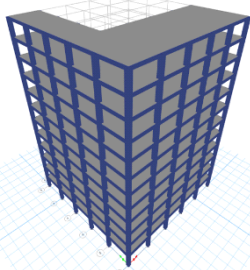
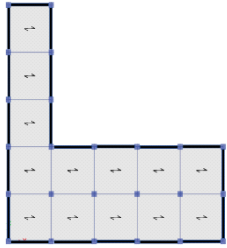
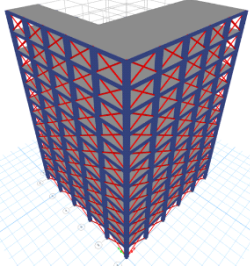
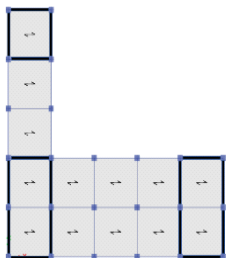
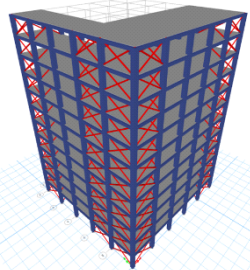
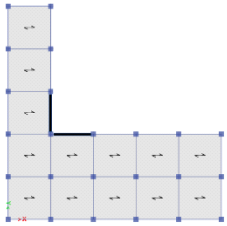
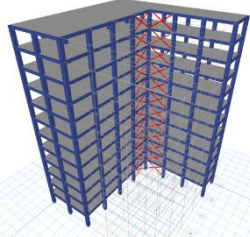
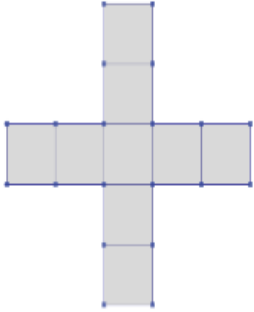
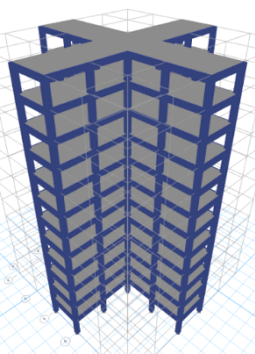


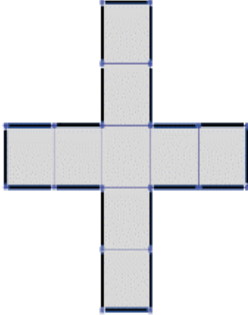
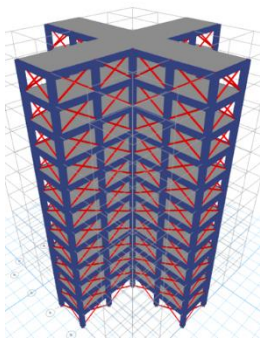
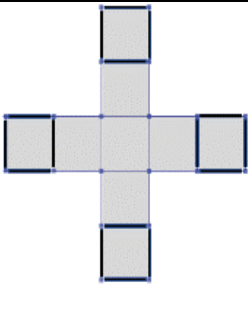
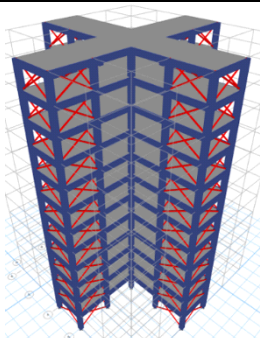
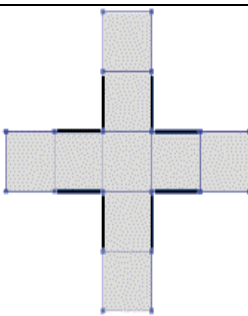
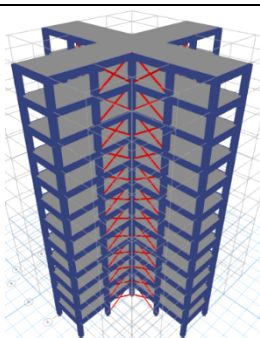
Fig. 4 Stress-strain diagram definition in ETABS for a) concrete and b) steel

Table 3 Plans, 3D views, and braces position of proposed buildings

Models	Plan view	3D view
M1		
M2		

M3		
M4		
M5		
M6		
M7		

M8		
M9		
M10		
M11		
M12		
M13		

M14		
M15		
M16		

### Methodology and analysis

The ETABS software was utilized for structural analysis and design [25]. This software is one of the most powerful and up-to-date finite element tools for structural analysis. It can estimate the significant displacement behavior of frames under static or dynamic loadings while accounting for geometric nonlinearities and material inelasticity. The software simulates the buckling of steel bracing and concrete confinement. It can run eight different types of analyses, including conventional and adaptive pushover analyses [30].

The behavior of G+11-story RC structures in irregular designs (I-, T-, L- and Plus-shapes) with different X-bracing locations is studied. For the design of these structures, the capacity design approach is applied. Godinez-Domínguez & Tena-Colunga (2019) [20] utilize a similar technique in the design of low to high-rise structures. The response spectrum method (RSM) is used to design the RC structures with steel bracing. The pushover analysis method is used to investigate the seismic behavior and structural strength of structures [27, 45]. For doing nonlinear analysis, it is necessary to consider the nonlinearities in the structure. The material nonlinearities are accounted for by assigning plastic hinges in beams, columns, and braces. M3 hinges are assigned at both ends

of all the beams. P-M2-M3 hinges are assigned at both ends of all columns and P(axial) hinges are assigned in the middle of all the braces. These nonlinear hinges are assigned according to ASCE 41-17 [10]. The geometric nonlinearity is considered by considering the P-delta effect on all the models. The formula suggested by ASCE 41-17 to calculate the target displacement ( $\delta_t$ ) is given by equation 4.

$$\delta_t = C_0 C_1 C_2 S_a \frac{T_e}{4\pi^2} g \quad (4)$$

Where:

$C_0$  = Modification factor to relate spectral displacement of an equivalent single-degree-of-freedom (SDOF) system to the roof displacement of the building multiple-degree-of-freedom (MDOF) system.

$C_1$  = Modification factor to relate expected maximum inelastic displacements to displacements calculated for the linear elastic response.

$C_2$  = Modification factor to represent the effect of pinched hysteresis shape, cyclic stiffness degradation, and strength deterioration on the maximum displacement response.

$S_a$  = Response spectrum acceleration at the effective fundamental period and damping ratio of the building in the direction under consideration.

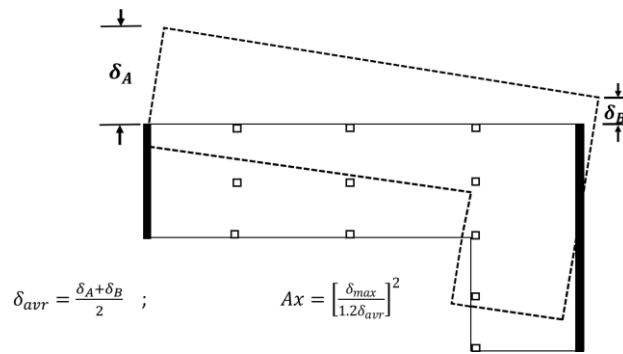
$g$  = Acceleration due to gravity.

To investigate the ductility characteristics of RC braced frames, capacity curves and plastic hinge formations are studied. The comparative research is designed to observe structural behaviors.

Re-entrant angle irregularity is defined as existing when both plan projections of the structure beyond a re-entrant angle are greater than 15% of the plan dimension of the structure in the given direction. To estimate the torsional irregularity of an L-shaped building, practically all seismic codes (RPA99/2003, UBC 97, ASCE 7-10 IS 1893:2016) have a comparable provision. The accidental impact torsion amplification factor  $A_x$  must be recognized for understanding [47]. The  $\delta_{max}$ ,  $\delta_{min}$ , and  $\delta_{avg}$  values represent the maximum, minimum, and average drift when the seismic load is applied from the x direction, as shown in Fig. 5. The torsional irregularity coefficient ( $\eta_t = \delta_{max}/\delta_{avg}$ ) is defined as the ratio of the maximum drift to the average drift. Three conditions are outlined:

- when  $\eta_t$  is less than or equal to 1.2, there is no torsional irregularity and  $A_x$  is equal to 1,
- when  $\eta_t$  is between 1.2 and 2.083, there is torsional irregularity, and  $A_x$  is calculated using the given formula (5), and
- when  $\eta_t$  is greater than 2.083,  $\eta_t = 2.083$  and  $A_x$  is equal to 3 [28].

$$A_x = \left[ \frac{\delta_{max}}{1.2\delta_{avr}} \right]^2 \quad (5)$$

Fig. 5 Torsional Amplification factor  $A_x$ 

## Results and discussion

In the ETABs software, 16 models with different X-bracing locations were analyzed first by using the RSA, and then the further study is carried out by using the nonlinear static analysis to observe the capacity of the structures. The various seismic parameters are observed such as Maximum story displacements, inter-story drifts, base shear, Fundamental time periods, story stiffness, torsional irregularity, Capacity curves, and plastic hinge formations to understand the effect of X-bracings in irregular shape RC buildings.

### Maximum story displacements

To analyze the seismic behavior of structures, one of the most important parameters is the maximum displacement. Due to increased drifts and displacements during earthquakes in high seismic zones, structures with irregular plan configurations sustain more severe damage than regular buildings. Therefore, if lateral deformations are controlled by giving a structure suitable lateral stiffness and strength, effective damage control may be accomplished [18].

**Figures 6 and 7** illustrate the variation of the story displacement for different models as a function of the number of stories in the X and Y directions. It was noted that the addition of steel bracing in different positions influenced the maximum displacements of the structures. The story displacements for the I-shaped models are shown in **Fig. 6 and 7 (a)**. Between models M1, M2, M3, and M4, model M2 has the minimum displacement, and model M1 has the maximum displacement at the roof level in both directions. The decrease in the story displacement for the M2 model is about 75% compared to the M1 model in the X-direction and about 78% in the Y-direction. Adding the steel bracing in the M4 model does not show as much effective control in the maximum displacements in both directions. For the T-shaped models, the M7 model shows the minimum displacement compared to other models in both directions as shown in **Fig. 6 and 7(b)**. The maximum story displacement is shown by the M5 model which is 60.17% more than the M7 model in the X-direction, and for the Y-direction we can observe that the M8 has the maximum story displacement which is 60.05% more than the M7 model and 9.36 % more than M5 model. The story displacements for the L-shaped models are shown in **Fig. 6 and 7 (c)**. We can see that the M10 has the minimum displacement compared to other models in the X-direction. But in the Y-direction we can observe that the minimum displacement goes to the M11 model which is 91.59 % less than the M12 and 90.37% less than the M9 model, and the maximum goes



to the M12 12.68% more than M9. For the Plus-shaped models, the M14 model shows the minimum displacement compared to other models in the X-direction as shown in Fig. 6(d). In the Y-direction the maximum value goes to the M13 and M16 models which are almost the same, and the minimum displacement shows in the M14 and M15 models which are 36.97% less than the two other models as shown in Fig. 7(d). From the results, it is understandable that the decrease in the number of bracings used (M2, M6, M10, and M14 models) is effective to reduce the story displacements in irregular shape structures [9, 34].

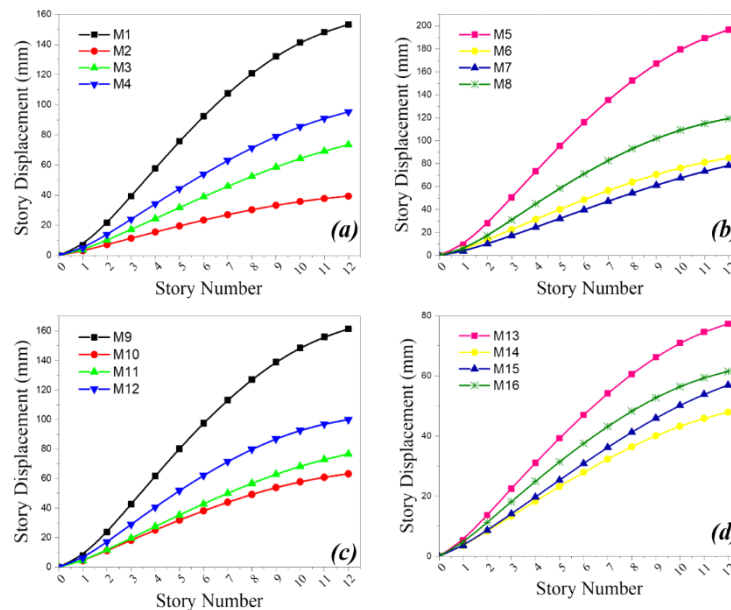


Fig. 6 Story displacement of different models along X-direction, (a) I shape (b) T shape (c) L shape (d) Plus shape.

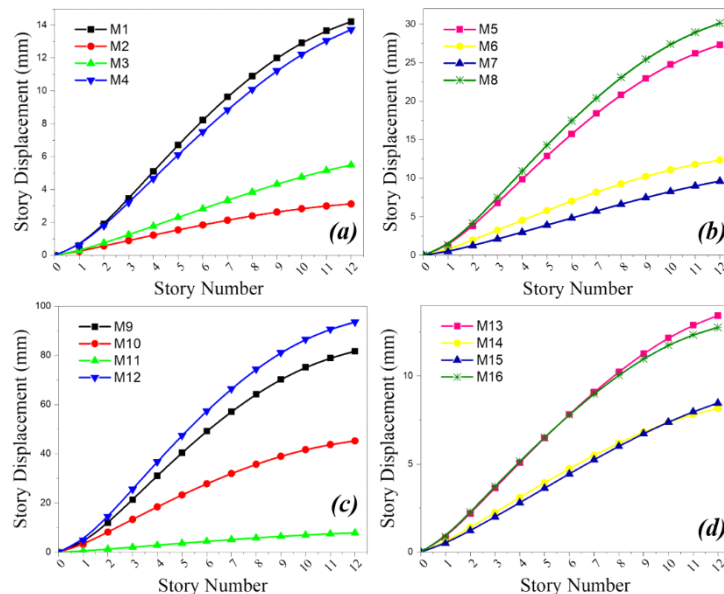


Fig. 7 Story displacement of different models along Y-direction, (a) I shape (b) T shape (c) L shape (d) Plus shape.

### • Inter-story drifts

The inter-story drift ratio is computed by dividing the relative translational displacement between two successive floors by the height of the stories. The safety of both structural and non-structural parts of a structure depends heavily on the control of the inter-story drift ratios. Fig. 8 and 9 show the inter-story drift ratios for all the models. The inter-story drift ratios over the height of the building for different models subjected to earthquake load increase non-linearly (parabolic manner) over the height of the building and reaches their maximum value in the fourth story level, then decreased towards higher levels for all shapes except the plus-shape reaches its maximum value in the third story level, in both directions. For the I-shaped models, the inter-story drift ratio response attains its minimum value in the M2 model which is 72.7% and 77.9%, respectively less than that of the M1 model in both X and Y-directions. In the T-shaped models, the inter-story drift ratio response attains its minimum value in the M7 model in both directions. For the L-shaped models in the X-direction, the M10 is the minimum value, but in the Y-direction we can see that the M11 is the minimum value. In the plus-shaped models, we can observe that M15 is the minimum value in both directions. From the results, The story drift in T-shaped building is greater than all other irregular buildings, and the Plus-shaped is lesser than others[46].

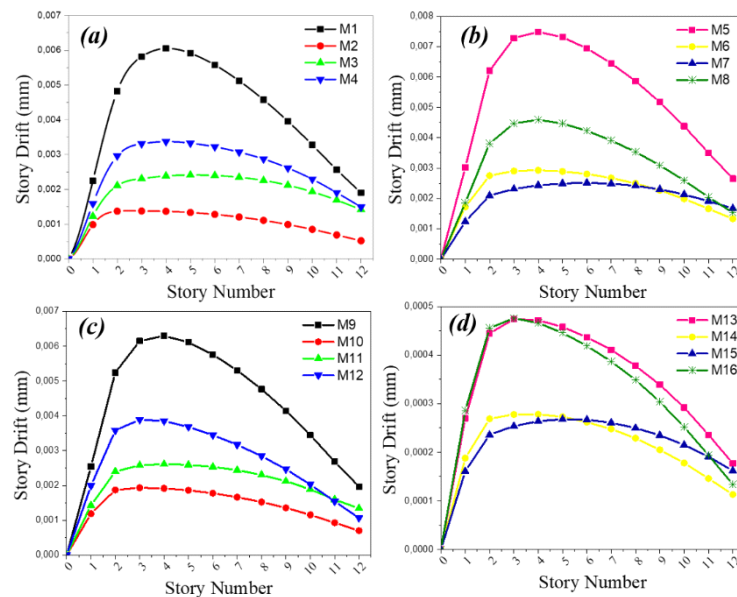


Fig. 8 Inter-story drift of different models along X-direction, (a) I shape (b) T shape (c) L shape (d) Plus shape.



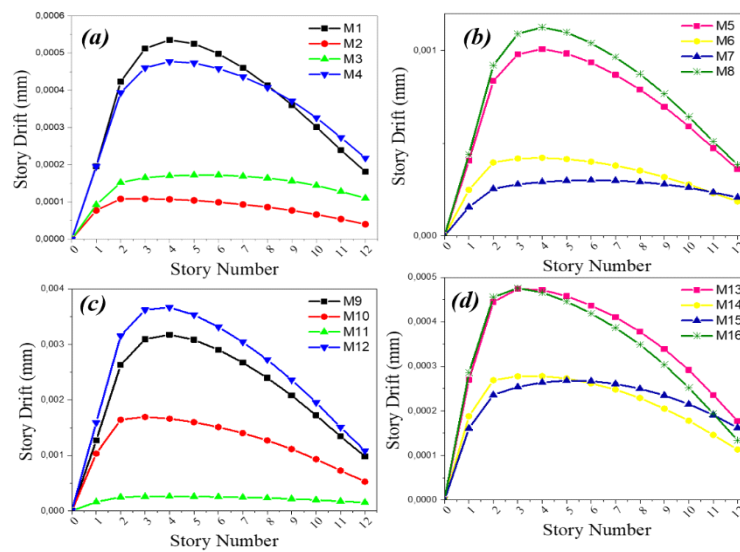


Fig. 9 Inter-story drift of different models along Y-direction, (a) I shape (b) T shape (c) L shape (d) Plus shape.

#### • Base shear

Base shear is a computation of the greatest lateral force that is anticipated to result from seismic ground motion at the base of the building. Asymmetry in the building's layout or lateral-torsional coupling phenomena both have an impact on the base shear. Adding bracing to existing structures effectively improved the structure's lateral shear-resisting capability. The use of bracing in RC frames raises the requirement for base shear in the overall constructions. The addition of steel bracings, on the other hand, improves the rigidity of the structures. The values of base shear obtained from the analysis in both directions are shown in fig.10 and 11. It is noticed that adding steel bracings raises the structure's base shear values, and comparable findings are reported in [16, 9], and [17]. In both the X and Y directions, the base shear in the T-shaped (M8) structure is smaller than that of any other irregular shapes. As a result, I-shaped (M2) buildings perform better in the X direction, whereas L-shaped (M10) buildings perform better in the Y direction.

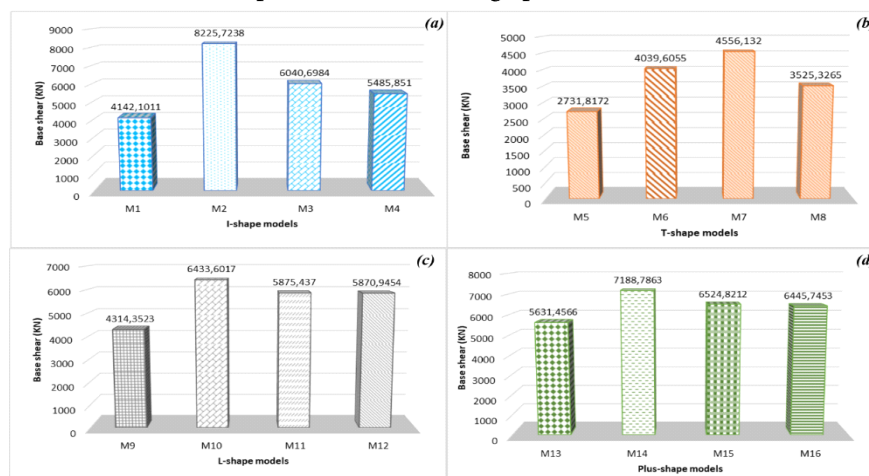


Fig. 10 Base shear of different models along X-direction, (a) I shape (b) T shape (c) L shape (d) Plus shape.

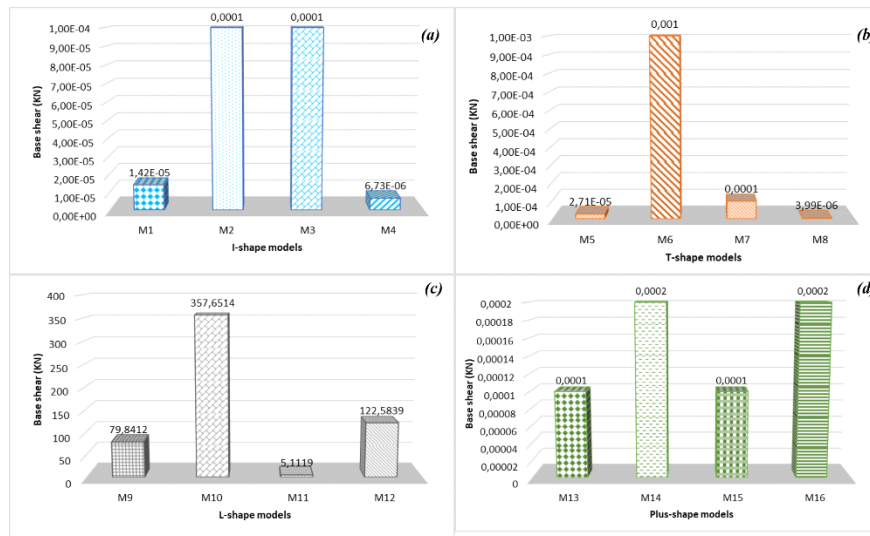


Fig. 11 Base shear of different models along Y-direction, (a) I shape (b) T shape (c) L shape (d) Plus shape.

### Fundamental time periods

The overall seismic requirements of structures are determined by the structure's fundamental time period. Several codes specify an empirical formula that is a function of building height. The formula, unfortunately, is only for regular structures and doesn't offer correct FTP for structures that are irregular and braced [18, 29]. Fig 12 shows the variation of the fundamental time periods of all models. It is obvious that when steel bracings are utilized in all bays of the structure (M2, M6, M10, M14), the fundamental time period of the structures is reduced and seen to be the shortest in the M14 model (Plus-shape).

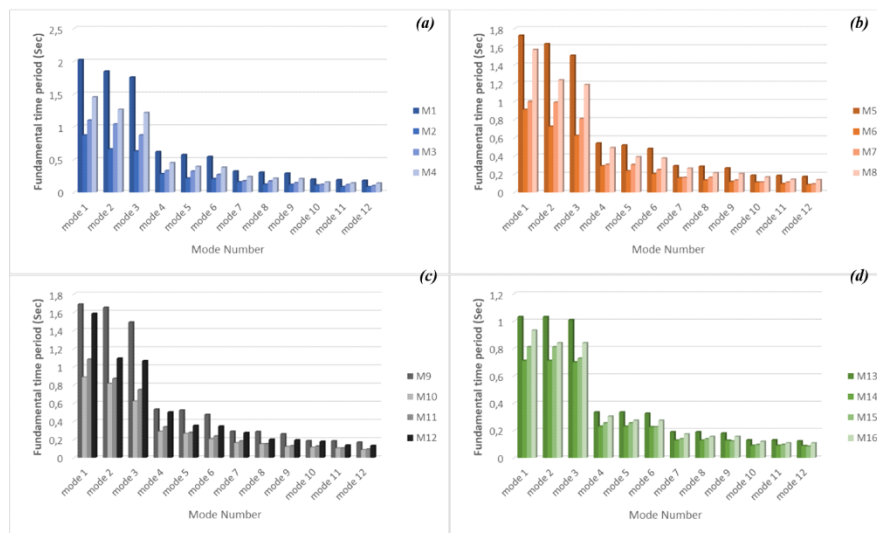


Fig. 12 Fundamental time periods of different models, (a) I shape (b) T shape (c) L shape (d) Plus shape.

- Story stiffness response

The degree of stiffness in the structures' stories depends on the size, shape, and length of the columns and bracings. The variance in story stiffness for each model is shown in Fig.13 in both X and Y-directions. Of all models, the M2 model has the maximum story stiffness value and the M5

model has the minimum one in the X-directions. The increase in the story stiffness for the M2 model is about 77.99% compared to the M1 model, similarly for M6, M10, and M14 story stiffness increased by 65.24%, 64.25%, and 48.20% times of M5, M9, and M13 respectively along the X-direction. Along the Y-direction, the maximum story stiffness is observed in the M14 model, and the minimum in the M9 model. The increase in the M14 model is about 48.21% compared to the M13 model, similarly for M2, M6, and M11 story stiffness increased by 70.19%, 71.47%, and 88.34% times of M1, M5, and M9 respectively along the Y-direction. It is noted that the addition of steel bracing in all bays of the structure, increases the story stiffness of the buildings.

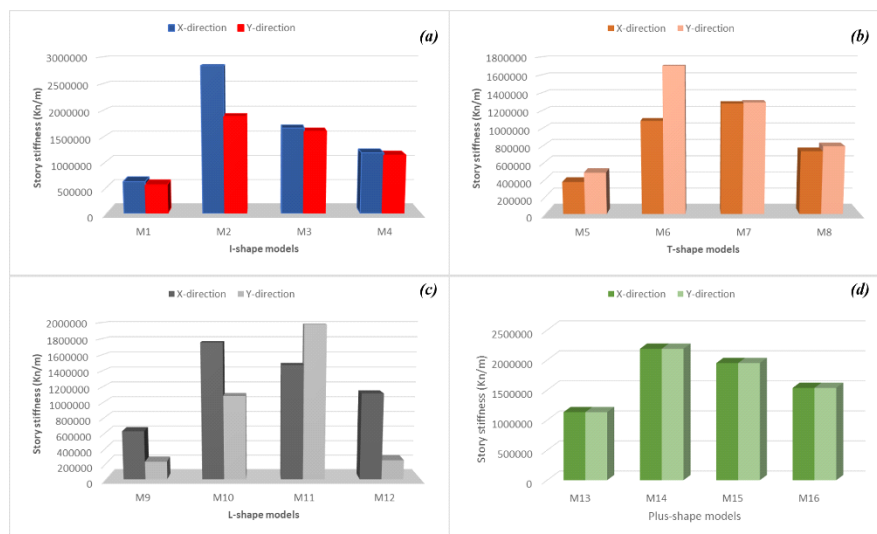


Fig. 13 Story stiffness response of different models, in X and Y-directions, (a) I shape (b) T shape (c) L shape (d) Plus shape.

#### • Torsional Irregularity Ratio

Torsional irregularity is one of the most critical characteristics influencing possible damage to building structures. The torsional irregularity ratio is defined as the maximum story drift, including accidental torsion, at the end of a structure transverse to an axis being greater than 1.2 times the average inter-story drift at the end of the structure [5, 15] and [22]. Furthermore, the torsional irregularity ratio is an analytical index developed from seismic response characteristics that account for the multi-directionality of earthquake movements as well as structural asymmetry. As a result, it captures the real three-dimensional inelastic factors that control building structure response, while also recognizing differential deformation in the plan, and hence the capacity of a vertical resisting element to tolerate expected lateral forces. Fig. 14 and 15 display the torsional irregularity ratio of different building models as a function of model height. The trends in the graph show that for all building models, the torsional irregularity varies slightly with the height of the building, while the value increases with increasing plane irregularity. The maximum torsional irregularity ratio when the unidirectional spectrum is used along the X-direction are 1.935, 1.067, 1.659, and 1.551 for the models M5, M6, M9, and M10 respectively. It is observed that model

M5 shows the maximum torsional irregularity ratio. However, for I and Plus-shapes, all the models show the safe torsional irregularity ratio (less than 1.2). In the L-shaped models, M9, M10, and M12 have torsional irregularity ratios greater than 1.2 along both X and Y-directions (see Fig. 14 and 15 (c)). The models M5, and M9, along the X and Y directions, further studied the torsional amplification factors because the models have the greatest torsional irregularity ratio ( $>1.2$ ). Table 4(a-b) and 5(a-b) shows the amplification factors for these models and the torsional amplification factors are greater than 1 and less than 3. Other models M7, M8, and M11 show better torsional behavior within limits. Models M7, M11, M6, M8, and M11 have provided a suitable bracing along the X and Y directions. The results also display that with the increase in plan irregularity of models, the maximum torsional irregularity ratio values increase and tend to reach the upper code limit value of 1.2.

When appropriately placed bracings are used, irregularly shaped RC structures exhibit favorable seismic characteristics and exhibit minimal displacements and drifts, and torsionally secure.

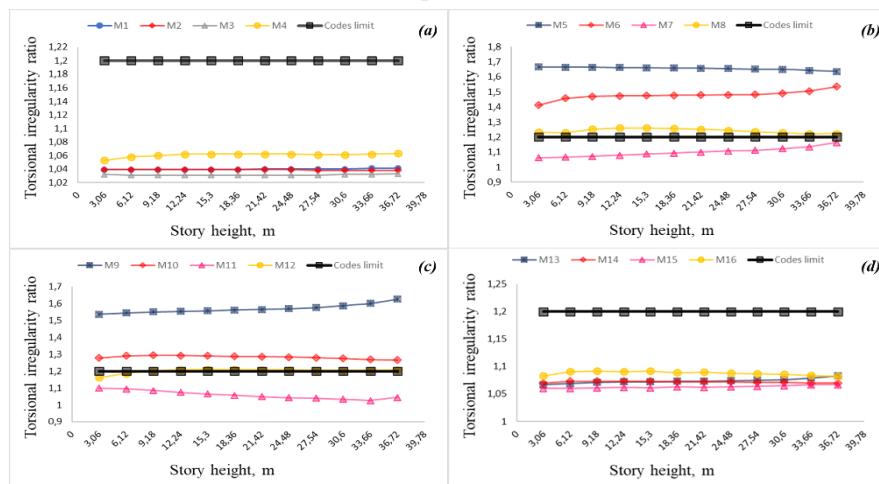


Fig. 14 Torsional irregularity ratio of different models along with height, in X-direction, (a) I shape (b) T shape (c) L shape (d) Plus shape.

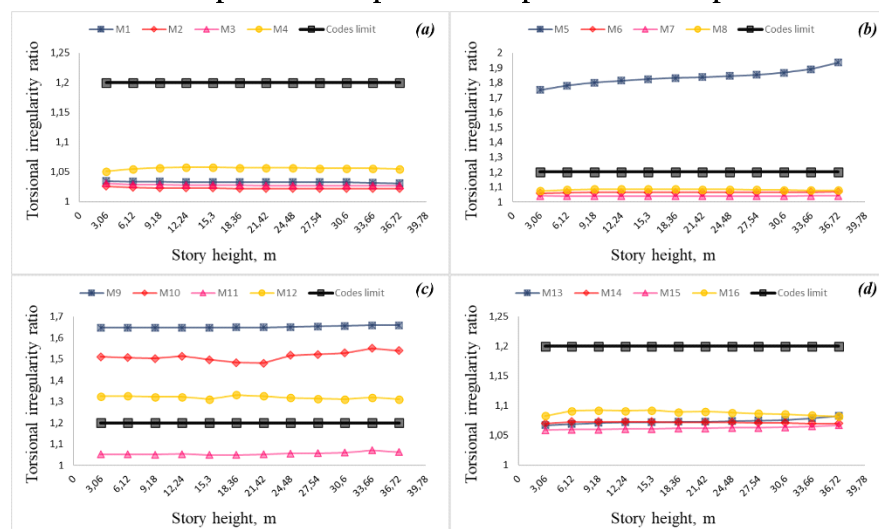


Fig. 15 Torsional irregularity ratio of different models along with height, in Y-direction, (a) I shape (b) T shape (c) L shape (d) Plus shape.

Table 4a. Calculation of torsional irregularity and torsional amplification factors for M5 along X-direction.

(mm)	(mm)	$\eta_t =$ /	$A_x$
0,001283	0,000784	1,041	1,8587
0,001696	0,001032	1,041	1,8746
0,002135	0,001295	1,04	1,8883
0,002536	0,001535	1,04	1,8952
0,002886	0,001744	1,04	1,9021
0,003185	0,001922	1,04	1,9067
0,003433	0,00207	1,039	1,9113
0,003623	0,002182	1,039	1,9136
0,003718	0,002237	1,039	1,9182
0,003625	0,00218	1,039	1,9205
0,003102	0,001864	1,039	1,9228
0,001526	0,000917	1,039	1,9252

Table 4b. Calculation of torsional irregularity and torsional amplification factors for M5 along the Y-direction.

(mm)	(mm)	$\eta_t =$ /	$A_x$
0,00036	0,000186	1,935	2,6002
0,000473	0,00025	1,891	2,4833
0,00059	0,000316	1,867	2,4206
0,000697	0,000376	1,853	2,3845
0,00079	0,000428	1,845	2,3639
0,000869	0,000473	1,838	2,3460
0,000935	0,000511	1,831	2,3282
0,000984	0,00054	1,823	2,3079
0,001008	0,000555	1,814	2,2851
0,000979	0,000544	1,801	2,2525
0,000835	0,000469	1,781	2,2028
0,000407	0,000233	1,752	2,1316

Table 5a. Calculation of torsional irregularity and torsional amplification factors for M9 along X-direction.

(mm)	(mm)	$\eta_t =$ /	$A_x$
0,000674	0,000414	1,626	1,8360
0,000896	0,000559	1,601	1,7800
0,001144	0,000722	1,586	1,7468
0,00138	0,000876	1,576	1,7248

0,00159	0,001013	1,569	1,7096
0,001773	0,001133	1,565	1,7009
0,001925	0,001234	1,561	1,6922
0,00204	0,00131	1,557	1,6835
0,002094	0,001348	1,554	1,6770
0,00203	0,00131	1,55	1,6684
0,001716	0,001111	1,544	1,6555
0,000828	0,000539	1,537	1,6405

**Table 5b. Calculation of torsional irregularity and torsional amplification factors for M9 along the Y-direction.**

(mm)	(mm)	$\eta_t = \frac{\Delta u_t}{\Delta u_b}$	$A_x$
0,000983	0,000593	1,658	1,9090
0,001341	0,000808	1,659	1,9113
0,001724	0,001041	1,656	1,9044
0,00208	0,001259	1,653	1,8975
0,002397	0,001453	1,65	1,8906
0,002672	0,001621	1,648	1,8860
0,002905	0,001764	1,647	1,8838
0,003084	0,001873	1,647	1,8838
0,003175	0,001928	1,647	1,8838
0,003094	0,001877	1,648	1,8860
0,002629	0,001594	1,649	1,8883
0,001271	0,000771	1,649	1,8883

### Pushover analysis

The pushover analysis is a non-linear static analysis generally used to study the capacity and overstrength of existing structures. In the retrofit process, the failure criteria of beams and columns should be observed. The pushover analysis is performed in the finite element software ETABS. The displacements-controlled method is used and the lateral load pattern is based on the fundamental mode shapes at each story level with corresponding story weights. The performance point or target displacements are obtained by using the displacements coefficients method by using the ASCE 41-17 [10]. The plastic hinges in beams, columns, and braces are defined. M3 hinges are assigned at both ends of all the beams. P-M2-M3 hinges are assigned at both ends of all columns and P (axial) hinges are assigned in the middle of all the braces. The lateral load is raised, and the lateral shear force and displacements are recorded and prepared for the pushover curve or capacity curve. The pushover analysis aids in understanding the structural capacity and failure prediction by predicting weak spots. The approach is usually employed in the retrofitting procedure. Fig.16 and 17 show the capacity curves of all models along the both X and Y- directions. Of all the models,

the capacity curves of unbraced structures (M1, M5, M9, and M13) lie under the capacity curves of other models in both directions. This behavior shows that the unbraced structures have less effective stiffness among all the models. On the other hand, it is noticed that adding the steel bracing in the RC frame structures, increases the strength capacity of the structures. The maximum increase in the effective stiffness for I, T, L, and plus-shapes is 18.55%, 30.97%, 37.48%, and 27.75% for M2, M6, M10, and M16 respectively in the X-direction, and about the Y-direction the maximum increase for M2, M6, M11, and M14 is about 21.54%, 22.38%, 26.75, and 21.85% respectively.

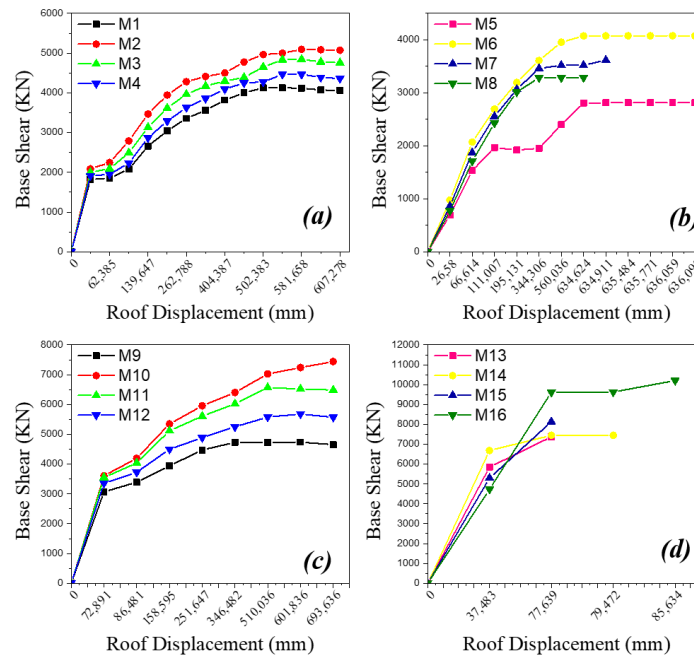


Fig. 16 Capacity curves of different models along X-direction, (a) I shape (b) T shape (c) L shape (d) Plus shape.

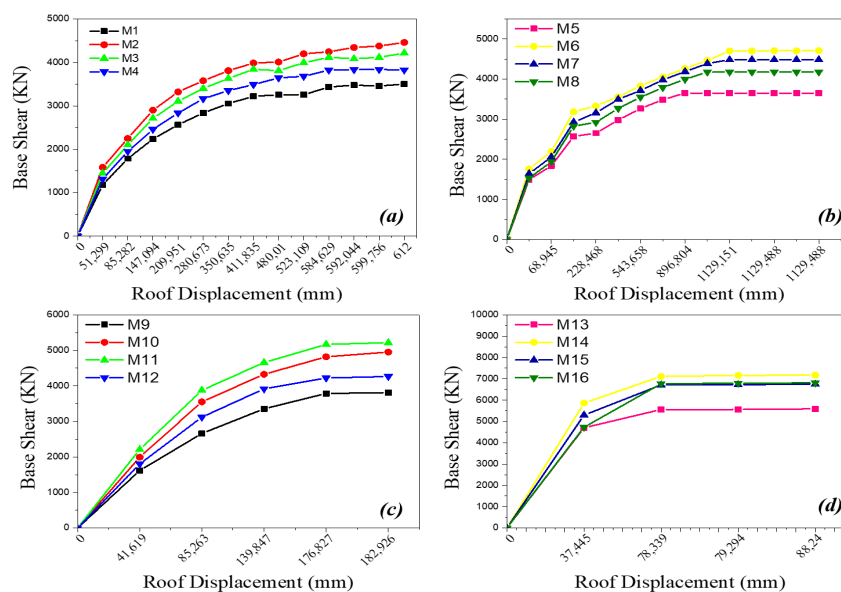


Fig. 17 Capacity curves of different models along Y-direction, (a) I shape (b) T shape (c) L shape (d) Plus shape.

Table 5a and 5b shows the target displacements obtained from the nonlinear static analysis in the X and Y directions. The M2, M6, M11, and M16 models show the maximum target displacement compared to all I, T, L, and plus-shaped models in the X-direction. This is due to the increased stiffness of the structures. For the T, and Plus-shaped structures M5, and M13 models, the target displacements could not be found in the X-direction for the given seismic hazard, and for the Y-direction the maximum target displacement is found in the M3, M6, M10, and M16 models for I, T, L, and plus-shapes structures. And in the plus-shape structure of the models M13, M14, and M15 the target displacements could not be found in the Y-direction for the given seismic hazard.

**Table 6a. Results of nonlinear static analysis of all models in the X-direction.**

Model	C0	C1	C2	$K_i=K_e$ (KN/m)	$\Delta_{max}$ (mm)	$V_b$ (KN)	$T_i=T_e$ (sec)
M1	1,275091	1	1	29826,46	361,636	3666,627	1,802
M2	1,374847	1	1	34108,709	374,777	4459,77	1,734
M3	1,344884	1	1	32685,092	371,111	4253,3073	1,754
M4	1,305181	1	1	31273,535	365,521	3978,37	1,777
M5	Target displacement could not be found						
M6	1,107928	1	1	36741,045	300,018	3487,8437	1,691
M7	1,058284	1	1	35689,235	292,931	3242,9691	1,729
M8	1,006477	1	1	34485,52	285,028	3007,1586	1,768
M9	1,441098	1	1	42526,651	437,034	5202,4466	1,923
M10	1,480258	1	1	47352,837	436,285	6122,1423	1,869
M11	1,507766	1	1	49500,778	439,282	6478,1532	1,848
M12	1,457559	1	1	45065,836	435,161	5679,5775	1,893
M13	Target displacement could not be found						
M14	1,143895	1,094289	1	305935,928	52,435	15372,5314	0,914
M15	0,398523	1,085782	1	450960,287	26,322	12132,0682	0,948
M16	1,692683	1	1	126327,58	282,79	10204,8494	1,06

**Table 6b. Results of nonlinear static analysis of all models in the Y-direction.**

Model	C0	C1	C2	$K_i=K_e$ (KN/m)	$\Delta_{max}$ (mm)	$V_b$ (KN)	$T_i=T_e$ (sec)
M1	1,308823	1	1	24355,023	410,494	3233,4676	1,995
M2	1,406682	1	1	28178,307	421,386	3989,237	1,902
M3	1,381935	1	1	26888,355	421,468	3754,3709	1,935
M4	1,350331	1	1	25625,899	419,069	3505,6595	1,968
M5	1,247313	1	1	28373,028	311,206	2813,3706	1,588
M6	1,31526	1	1	32640,367	317,209	3571,5901	1,53
M7	1,289021	1	1	31296,651	313,177	3346,9664	1,546
M8	1,266111	1	1	29894,758	312,05	3097,3564	1,564



M9	0,378421	1,28763	1	47925,379	69,237	2995,1478	0,888
M10	0,453174	1,216492	1	40814,728	86,189	2834,55	0,978
M11	0,400352	1,286126	1	45680,628	74,985	2976,387	0,911
M12	0,431816	1,279178	1	43342,104	82,978	3053,2599	0,94
M13	Target displacement could not be found						
M14	Target displacement could not be found						
M15	Target displacement could not be found						
M16	0,616622	1,175733	1,059255	126330,587	79,805	9821,6344	0,653

Fig.18 and 19 show the plastic hinge formation in the un-braced I, T, and L-shaped structures. At the target displacements, none of the models showed non-linear behavior. None of the plastic hinges assigned to columns, braces, and beams crossed immediate occupancy (IO) performance levels at the obtained target levels, except for the unbraced models, where the plastic hinges assigned to columns passed the collapse prevention (CP) and some beams crossed life safety (LS) performance levels in both the X and Y directions. Similar observations were also observed in the previous study for X bracings [20].

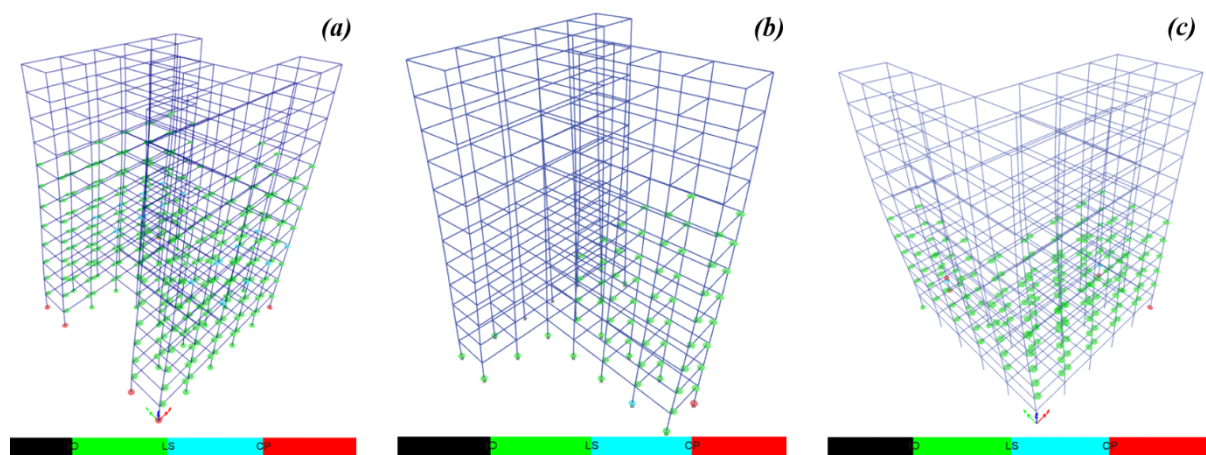


Fig. 18 Plastic hinge formation of different models along X-direction, (a) I shape (b) T shape (c) L shape.

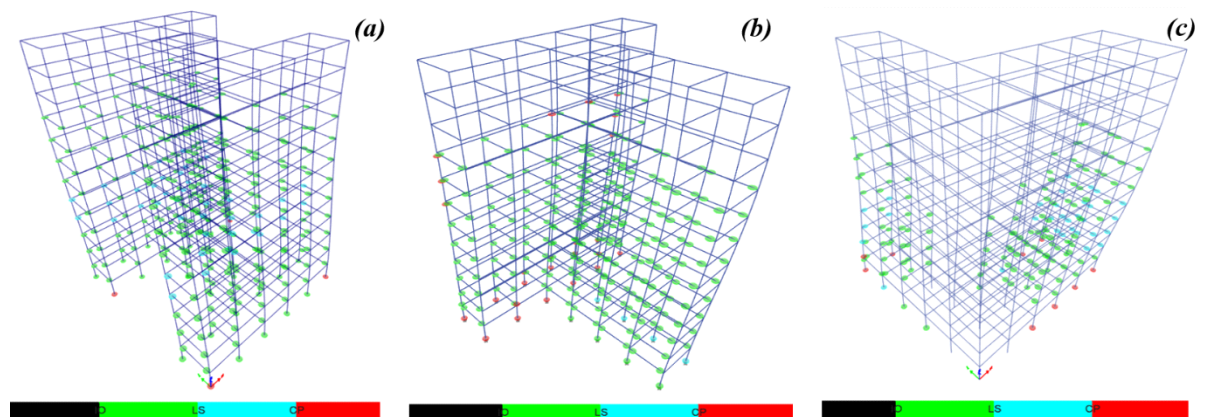


Fig. 19 Plastic hinge formation of different models along Y-direction, (a) I shape (b) T shape (c) L shape.

**Conclusions**

In this study, an attempt is made to find the most effective position of X-bracing in different irregularly shaped structures. The RC structures are modeled and analyzed in four different shapes (I, T, L, and PLUS-shapes) by performing nonlinear static analysis. A total of 16 models are analyzed. The main conclusions obtained from this study are as follows:

- [1] From the results plotted in the form of story displacements and inter-story drifts ratios, it can be concluded that providing the steel bracings in the irregularly shaped RC buildings, reduced the maximum displacements and the inter-story drift in the buildings. The M2, M7, M10, and M14 models show the effective reduction of maximum displacements and inter-story drift in both directions. It is noticed that nearly 70% reductions in maximum displacements and inter-story drift are observed as compared to the unbraced models. If the bracings are provided symmetrically, it reduces the maximum displacements properly with a minimum torsional effect.
- [2] When investigating the influence of different positions of X-bracing in RC structures, it was discovered that when steel bracing is utilized, the lateral base shear value increases in irregular buildings. The base shear value increases as the number of braced bays grows in both directions, especially in M2, M6, M10, and M14. When steel bracing is employed appropriately in irregular buildings, the fundamental time period of the structures is reduced.
- [3] Steel bracings in irregular-shaped buildings efficiently improve the story stiffness of the structures. When the number of bays is increased, the stiffness of the structures increases.
- [4] The torsional irregularity ratio is investigated in both X and Y directions of all models, and it is discovered that M6 and M8 in the T-shape models, and M10 and M12 in the L-shape models, exhibit an unanticipated torsional effect. All Plus-shape and I-shape models, on the other hand, display good seismic performance. M7 and M11 show the accepted torsional irregularity ratio in both directions. The torsional irregularity ratio should be evaluated carefully when utilizing steel bracing in an irregular building.
- [5] From the pushover analysis, it can be concluded that the installation of steel bracing in irregularly shaped structures increases the capacity and ductility of these structures compared to unbraced ones. And the failure mechanism gets more regular as well.
- [6] From the analysis, it can be concluded that (M2, M7, M10, and M14) bracing positions can be used to minimize the damage under seismic forces effectively.
- [7] The worst behavior is shown for the (M4, M8, M12, and M16) bracing position. They show higher story displacements, inter-story drift ratios, time period, low effective stiffness, and base shear. This shows that these bracing positions are not very effective in reducing the seismic responses of irregular structures.
- [8] In general, retrofitting irregular 12-shape RC structures with different positions of X-bracing is helpful to the structure if the steel bracing positions (M2, M7, M10, and M14) are properly utilized.

This study examines the influence of different X-bracing placements in an irregularly shaped RC structure using nonlinear static analysis. As a result, the findings of this study are confined to this particular situation. However, more research with nonlinear dynamic analysis with alternative bracing arrangements and placements in other forms of irregularities is required. It's also vital to investigate the interactions of columns and steel bracing connections, as well as their impact on the entire structure's behavior.

## References

- [1] F. C. Dya and A. W. C. Oretaa, "Seismic vulnerability assessment of soft story irregular buildings using pushover analysis," *Procedia Eng.*, vol. 125, pp. 925–932, 2015.
- [2] Faisal, T. A. Majid, and G. D. Hatzigeorgiou, "Investigation of story ductility demands of inelastic concrete frames subjected to repeated earthquakes," *Soil Dyn. Earthq. Eng.*, vol. 44, pp. 42–53, 2013.
- [3] Formisano, A. Massimilla, G. Di Lorenzo, and R. Landolfo, "Seismic retrofit of gravity load designed RC buildings using external steel concentric bracing systems," *Eng. Fail. Anal.*, vol. 111, p. 104485, 2020.
- [4] Gottala, K. S. N. Kishore, and S. Yajdhani, "Comparative study of static and dynamic seismic analysis of a multistoried building," *IJSTE-International J. Sci. Technol. Eng.*, vol. 2, no. 01, 2015.
- [5] Guide, A. Manual, and A. P. I. RP, "ACI 318, Building Code Requirements for Structural Concrete (ACI 318-05) and Commentary (ACI 318R-05), ACI Committee 318, American Concrete Institute, Farmington Hills, MI, 2005 ACI 530, Building Code Requirements for Masonry Structures (ACI 530-05/ASCE 5)".
- [6] J. Kappos and S. Stefanidou, "A deformation-based seismic design method for 3D R/C irregular buildings using inelastic dynamic analysis," *Bull. Earthq. Eng.*, vol. 8, no. 4, pp. 875–895, 2010.
- [7] K. Chopra and R. K. Goel, "A modal pushover analysis procedure to estimate seismic demands for unsymmetric-plan buildings: theory and preliminary evaluation," *Earthq. Eng. Res. Cent.*, 2003.
- [8] Rahimi and M. R. Maheri, "The effects of retrofitting RC frames by X-bracing on the seismic performance of columns," *Eng. Struct.*, vol. 173, pp. 813–830, 2018.
- [9] Rahimi and M. R. Maheri, "The effects of steel X-brace retrofitting of RC frames on the seismic performance of frames and their elements," *Eng. Struct.*, vol. 206, p. 110149, 2020.
- [10] S. of C. Engineers, "Seismic evaluation and retrofit of existing buildings," 2017.
- [11] Viji, S. A. Daniel, and A. S. Hameed, "Seismic performance of RC frame retrofitted using steel bracing . Rendimiento sísmico de la estructura de RC reacondicionada utilizando refuerzos de acero .," vol. 11, no. X, 2023.
- [12] Y. Alghuff, S. M. Shihada, and B. A. Tayeh, "Comparative study of static and response spectrum methods for seismic analysis of regular RC buildings," *J. Appl. Sci.*, vol. 19, no. 5,

- [13] B. Anuse and K. Shinde, "Analysis of RC Irregular Building According to Different Seismic Design Codes," *Trends Civ. Eng. Challenges Sustain.*, pp. 239–248, 2021.
- [14] B. Bagheri, E. S. Firoozabad, and M. Yahyaei, "Comparative study of the static and dynamic analysis of multi-storey irregular building," *World Acad. Sci. Eng. Technol.*, vol. 6, no. 11, pp. 1847–1851, 2012.
- [15] B. I. S. IS, "Indian standard criteria for earthquake resistant design of structures: Part 1 general provisions and buildings," *Bur. Indian Stand.*, 2002.
- [16] B. K. Bohara, "Seismic Response of Hill Side Step-back RC Framed Buildings with Shear Wall and Bracing System," *Int. J. Struct. Constr. Eng.*, vol. 15, no. 4, pp. 204–210, 2021.
- [17] B. K. Bohara, K. H. Ganaie, and P. Saha, "Effect of position of steel bracing in L-shape reinforced concrete buildings under lateral loading," *Res. Eng. Struct. Mater.*, vol. 8, no. 1, pp. 155–177, 2022, doi: 10.17515/resm2021.295st0519.
- [18] B. Khanal and H. Chaulagain, "Seismic elastic performance of L-shaped building frames through plan irregularities," in *Structures*, 2020, vol. 27, pp. 22–36.
- [19] B. Standard, "Eurocode 2: Design of concrete structures—," Part 1, vol. 1, p. 230, 2004.
- [20] E. A. Godínez-Domínguez and A. Tena-Colunga, "Behavior of ductile steel X-braced RC frames in seismic zones," *Earthq. Eng. Eng. Vib.*, vol. 18, no. 4, pp. 845–869, 2019.
- [21] F. Pervez, F. A. Khan, B. Alam, F. Alam, and N. Ahmad, "Seismic performance of deficient reinforced concrete frames retrofitted with eccentric steel braces," *Innov. Infrastruct. Solut.*, vol. 7, no. 6, pp. 1–17, 2022.
- [22] G. Özmen, K. Girgin, and Y. Durgun, "Torsional irregularity in multi-story structures," *Int. J. Adv. Struct. Eng.*, vol. 6, no. 4, pp. 121–131, 2014.
- [23] H. E. Estekanchi, V. Valamanesh, and A. Vafai, "Application of endurance time method in linear seismic analysis," *Eng. Struct.*, vol. 29, no. 10, pp. 2551–2562, 2007.
- [24] Capanna, F. Di Fabio, and M. Fragiaco, "A simplified method for seismic assessment of unreinforced masonry buildings," *Civ. Eng. Environ. Syst.*, vol. 39, no. 1, pp. 66–91, 2022.
- [25] Computers and Structures, "CSI analysis reference manual for SAP2000, ETABS, and SAFE." Computers and Structures, Inc. Berkeley, CA, 2007.
- [26] K. H. Ganaie, B. K. Bohara, and P. Saha, "Effects of Inverted V Bracing in Four-Story Irregular Rc," *Int. Res. J. Mod. Eng. Technol. Sci.*, vol. 03, no. 04, pp. 2346–2351, 2021, [Online]. Available: [www.irjmets.com](http://www.irjmets.com)
- [27] K. H. Ganaie, B. K. Bohara, and P. Saha, "Effects Of Inverted V Bracing In Four-Story Irregular Rc Structures," *Int. Res. J. Mod. Eng. Technol. Sci.*, vol. 3, no. 04, pp. 2346–2351, 2021.
- [28] K. K. Sneha and J. Durgaprasad, "An Investigation of Coefficient of Torsional Irregularity for Irregular Buildings in Plan," in *Sustainability Trends and Challenges in Civil Engineering*, Springer, 2022, pp. 637–656.
- [29] M. M. M. Ahmed, S. E. Abdel Raheem, M. M. Ahmed, and A. G. A. Abdel Shafy, "Irregularity

effects on the seismic performance of L-shaped multi-story buildings,” JES. J. Eng. Sci., vol. 44, no. 5, pp. 513–536, 2016.

- [30] M. R. Maheri and A. Fathi, “The Effects of X-Brace Configuration on the Seismic Performance of Retrofitted RC Frames,” Iran. J. Sci. Technol. Trans. Civ. Eng., pp. 1–24, 2022.
- [31] M. R. Maheri and A. Sahebi, “Experimental investigation on the use of steel bracing in reinforced concrete frames,” in Proceedings of the Second International Conference on Seismic and Earthquake Engineering, Iran, 1995, vol. 1, pp. 775–784.
- [32] M. R. Maheri and A. Sahebi, “Use of steel bracing in reinforced concrete frames,” Eng. Struct., vol. 19, no. 12, pp. 1018–1024, 1997.
- [33] M. Sukrawa, “Staged analysis of rc frame retrofitted with steel braces in low and medium-rise buildings,” Procedia Eng., vol. 171, pp. 1002–1009, 2017.
- [34] M. Ubaid and R. A. Khan, “Performance Assessment of Vertically Irregular Steel Buckling-Restrained Braced Frame with Different Bracing Configurations,” in International Conference on Advances in Structural Mechanics and Applications, 2022, pp. 350–363.
- [35] M. V Landge and R. K. Ingle, “Tri-directional Floor Response Spectra in Irregular Building,” J. Inst. Eng. Ser. A, vol. 103, no. 1, pp. 57–69, 2022.
- [36] N. M. Abraham and A. K. SD, “Analysis of irregular structures under earthquake loads,” Procedia Struct. Integr., vol. 14, pp. 806–819, 2019.
- [37] P. A. Krishnan and N. Thasleen, “Seismic analysis of plan irregular RC building frames,” IOP Conf. Ser. Earth Environ. Sci., vol. 491, no. 1, 2020, doi: 10.1088/1755-1315/491/1/012021.
- [38] P. Agrawal and M. Shrikhande, Earthquake resistant design of structures. PHI Learning Pvt. Ltd., 2006.
- [39] P. Castaldo, E. Tubaldi, F. Selvi, and L. Gioiella, “Seismic performance of an existing RC structure retrofitted with buckling restrained braces,” J. Build. Eng., vol. 33, p. 101688, 2021.
- [40] P. Tehrani and M. Salari, “Seismic Performance of RC Buildings with Irregularities in Plan and Height, Retrofitted Using Steel Bracing,” Asas J., vol. 22, no. 61, 2021.
- [41] R. A. Oyguc and H. Boduroglu, “Seismic capacity assessment of existing irregular reinforced concrete (RC) buildings by an adaptive three-dimensional pushover procedure,” in 15th World conference on earthquake engineering, Lisbon, paper, 2012, no. 815.
- [42] R. P. Algériennes, “RPA 99/Version 2003,” Cent. Natl. Rech. Appliquée en Génie Parasismique, Algiers, Alger., 2003.
- [43] R. S. Banginwar, M. R. Vyawahare, and P. O. Modani, “Effect of plans configurations on the seismic behaviour of the structure by response spectrum method,” Int. J. Eng. Res. Appl, vol. 2, pp. 1439–1443, 2012.
- [44] S. K. Duggal, Earthquake resistant design of structures. Oxford university press New Delhi, 2007.
- [45] S. S. Farheen and B. Rohini, “Seismic Response of Multi-storey Building with Different Plan Configuration Using X-Bracing,” in Sustainability Trends and Challenges in Civil Engineering, Springer, 2022, pp. 963–978.

- [46] Sophia Merrin Saji and Sreedevi Lekshmi, “Comparison of Seismic Analysis of Chevron Bracings in Regular and Irregular Buildings,” *Int. J. Eng. Res.*, vol. V6, no. 06, 2017, doi: 10.17577/ijertv6is060269.
- [47] V. Alecci, M. De Stefano, S. Galassi, M. Lapi, and M. Orlando, “Evaluation of the American approach for detecting plan irregularity,” *Adv. Civ. Eng.*, vol. 2019, 2019.